ELSEVIER

Nuclear Instruments and Methods in Physics Research A 457 (2001) 447–453

NUCLEAR INSTRUMENTS & METHODS IN PHYSICS RESEARCH Section A

www.elsevier.nl/locate/nima

Wavelength-shifting fibers for calorimetric measurements in a long base line neutrino oscillation experiment

K.V. Alexandrov[a,b,c], G.C. Barbarino[a,b], P. Bernardini[d,e], M. Brigida[f,g], D. Campana[a,b], A. Candela[h], R. Caruso[a,b], F. Cassese[a,b], A. Ceres[f,g], B. D' Aquino[a,b], G. De Cataldo[f,g], I. De Mitri[d,e], A. Di Credico[h], C. Favuzzi[f,g], P. Fusco[f,g], F. Gargano[f,g,*], N. Giglietto[f,g], F. Giordano[f,g], A. Grillo[h], F. Guarino[a,b], C. Gustavino[h], E. Lamanna[i,j], A. Lauro[a,b], A. Leone[d,e], F. Loparco[f,g], G. Mancarella[d,e], D. Martello[d,e], M. N. Mazziotta[f,g,*], S. Mikheyev[h], M. Mongelli[f,g], G. Osteria[a,b], V. Palladino[a,b], G. Passeggio[a,b], M. Perchiazzi[f,g], G. Pontoniere[a,b], A. Rainò[f,g], R. Rocco[a,b], E. Romanucci[a,b], U. Rubizzo[a,b], A. Sacchetti[f,g], E. Scapparone[h], P. Spinelli[f,g], V. Tikhomirov[c], A. Vaccina[f,g], E. Vanzanella[a,b], M. Weber[a,b]

[a] *Dipartimento di Scienze Fisiche dell' Università di Napoli, Italy*
[b] *INFN Sez. di Napoli, Italy*
[c] *P.N. Lebedev Physical Institute, Moscow, Russia*
[d] *Dipartimento di Fisica dell' Università di Lecce, Italy*
[e] *INFN Sez. di Lecce, Italy*
[f] *Dipartimento di Fisica dell'Università di Bari, Via Amendola 173, I-70126 Bari, Italy*
[g] *INFN Sez. di Bari, Italy*
[h] *Laboratori Nazionali di Gran Sasso,INFN, Assergi (AQ), Italy*
[i] *Dipartimento di Fisica dell'Università della Calabria, Rende (CS) Italy*
[j] *INFN, Italy*

Received 2 May 2000; accepted 26 June 2000

Abstract

The NOE Collaboration has proposed a calorimeter to measure the energy of the final states of ν interaction events. The properties of long scintillator bars with wavelength-shifting fiber readout have been studied to develop a calorimeter design option. Various prototypes have been exposed to a cosmic rays stand.

The total measured light yield in the middle of a 6 m-long fiber is about 15 photoelectrons. With this photon collection performance, it has been simulated that the calorimeter can achieve $17\%/\sqrt{E}$ and $50\%/\sqrt{E}$ resolutions for electrons and pions, respectively.

1. Introduction

After the SuperKamiokande [1], MACRO [2] and Soudan2 [3] results reporting evidence for

* Corrresponding authors. Fax: +39-080-544-2470.
E-mail addresses: gargano@ba.infn.it (F. Gargano), mazziotta@ba.infn.it (M.N. Mazziotta).

0168-9002/01/$ - see front matter
PII: S0168-9002(00)00781-6

neutrino oscillation, a new generation of Long Base Line (LBL) and atmospheric neutrino experiments is being discussed. Several experiments have been recently proposed: ICANOE [4], MINOS [5], MONOLITH [6], NICE, OPERA [7] and K2K [8], that is the only one already yielding data. Both LBL and atmospheric neutrino experiments are foreseen to run underground, where the available space is limited. In addition, neutrino physics requires massive detectors, in order to compensate for the low neutrino cross-section, therefore demanding an efficient space use. As a consequence, the transverse dimensions of the detectors have to fill a relevant part of the underground halls. On the other hand, neutrino experiments require good calorimetric performance to reconstruct the incoming neutrino energy and to provide an efficient beam monitor.

In NOE proposal [9] we present our program to search for ν_μ oscillation by detecting the appearance of ν_τ (by the identification of τ decays) as well as the appearance of ν_e (by measuring an excess of events with an electron in the final state). We search also for the disappearance of ν_μ by measuring an increase of the neutral current (NC) to the charged current (CC) ratio. In case of large Δm^2 (beyond $\Delta m^2 = 5 \times 10^{-3}$ eV^2), besides the search of ν_τ appearance via kinematical cuts, ν_μ energy distribution due to oscillation could be observed with adequate statistics.

The detector has been tailored to get a high sensitivity to ν_τ, ν_e appearance at the CNGS [10] energies (~ 20 GeV on the average) by improving at best its tracking capabilities and energy resolution. The basic detector module is based on an instrumented target capable of particle identification, followed by a calorimeter and a muon detector. In this way two classes of events can be recorded. The first class includes neutrino interactions in both detectors where, through the muon identification, the ν_μ oscillation search is accomplished in the disappearance channel. The second one includes neutrino interactions in the first granular but massive device, where event vertex reconstruction, kinematical analysis, particle tracking and identification can be carried out. The downstream calorimeter fully contains the event and measures its total (and transverse) energy at a level of $20\%/\sqrt{E}$ for electrons and $50\%/\sqrt{E}$ for hadrons [9]. In this event sample, the appearance of ν_τ, ν_e oscillated events can be detected.

Recently, the ICARUS [11] and the NOE collaborations joined the ICANOE proposal, an appropriate combination of the ICARUS liquid argon imaging capability with the NOE fine grain calorimeter, suitably upgraded to provide also the magnetic analysis of muons. This new detector would address the detection of neutrinos coming from the CERN beam, of atmospheric neutrinos and searches for nucleon decays.

Neutrino physics claims large area detectors and in particular large area calorimeters. Nowadays these are essentially based on gas detector and scintillating fibers. Gas detectors with transverse dimension larger than 10 m have been used in several detectors: for instance, the MACRO experiment successfully used 12 m long streamer tubes [12]. Unfortunately, sampling calorimeters with this kind of gas detectors show a modest energy resolution, being strongly limited by the small energy sampling fraction [13]. Higher performance can be achieved by using plastic scintillator, but the main drawback comes from the small attenuation length ($\lambda \leq 2$ m). To face this problem a sampling calorimeter based on scintillating fibers has been built [14].

Actually, the ICANOE collaboration is studying the properties of scintillating fibers calorimeter [15] and has achieved an energy resolution of $43\%/\sqrt{E}$ for hadrons and $21\%/\sqrt{E}$ for electrons. Another interesting technique to face the problem of the small attenuation length is to couple solid scintillator bars to wavelength-shifting fibers, which capture the light emitted in the scintillator. Several meters of attenuation length can thus be obtained allowing both good energy resolution and reasonable detector transverse dimensions. This technique can considerably reduce the number of readout channels.

We have constructed and studied prototype detectors where the signal was collected from the scintillating fiber and delivered to high-gain photomultipliers (PMs). Our prototypes have been tested in a cosmic ray stand. We present in this paper the results in terms of photoelectrons yield, efficiency and attenuation length.

2. Prototype assembling

2.1. Scintillators

The prototypes have been built by using a commercially available plastic scintillator by Pol.Hi.Tech [16]. The main properties of this scintillator are an attenuation length of 4 m, an emission peak of 420 nm and a light yield of 35% of anthracene (Table 1).

The scintillators have been cut as 23 cm- and 600 cm-long bars having a cross-section of 1×4 cm^2 or 0.5×1 cm^2. On the top of this bars we milled a central square groove of 2.2×2.2 mm^2.

We have cleaned the bars with ethanol (40%) and de-ionized water (60%) solution to avoid any damage to the scintillator bulk. We have polished the machined surfaces with different abrasive papers. Later, a finer polishing has been performed, using an abrasive paste. We have left the central groove unpolished, to collect diffuse light from the scintillator onto the fiber.

2.2. WLS fibers

The used WLS single cladding fibers (Pol.Hi.Tech. S048) have a 2 mm diameter and are 600 cm long. Their main characteristics are summarized in Table 2.

Before assembling the prototypes, the fiber ends have been cut and polished by using a fine grain abrasive paper. We have taken particular care to prepare fiber end coupling to the PM windows to maximize the light transmission efficiency.

2.3. Assembly

We have placed the fiber inside the silicon oil-filled bar groove, to obtain a good optical matching. It has to be pointed out that, since light is totally reflected inside the fiber core, the silicon oil does not affect its transmission (Fig. 1). To keep the fiber in place, a thin plexiglass slab has been put over the scintillator bar. By firmly pushing the slab, the exceeding silicon oil has been removed.

We have wrapped the whole prototype with a white paper sheet in order to partially recover photons by diffuse reflection. Finally, it has been entirely wrapped with a sheet of thick black paper to ensure light tightening.

Table 1
Characteristics of the Pol.Hi.Tech. scintillator[a]

Scintillator	Pol.Hi.Tech
λ_{att}	4 m
λ_{emis}	420 nm
τ	2.5 ns
Light yield	35% anthracene $\rightarrow$ 2.0 p.e./mm/MIP

[a]Light yield is normalized to the light output of anthracene.

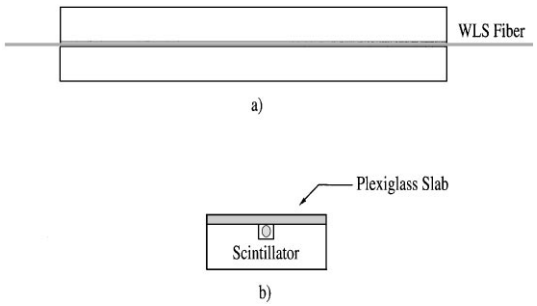

Fig. 1. Experimental setup: (a) top view, (b) front view.

The photomultiplier tube (PM) used to perform all the tests is the Philips XP2020. One of the ends of the WLS fiber was held within a plexiglass housing and then optically coupled with the PM photocathode window.

3. Data taking and analysis

3.1. Trigger

We have used a trigger to select cosmic rays crossing the tested prototype. It consists of two scintillating bars directly coupled with Philips XP2008 PMs, respectively, placed on the top and bottom of the prototype. The trigger layout is shown in Fig. 2.

The PM signals are discriminated by means of two LeCroy Octal Discriminators 4609C, with a 20 mV threshold. A logic coincidence of the two signals is carried out by means of a Caen 3-fold

Table 2
Main properties of the WLS single cladding fibers[a]

n_{core}	1.59
$n_{cladding}$	1.49
Cladding thickness	3.5% of the core diameter
Numerical opening	0.57
λ_{ass}	420 nm
λ_{emis}	481 nm

[a]The numerical opening is defined as $NO = n_{core} \cos \phi_c$ where ϕ_c is the critical angle.

Logic Unit N405. The output NIM signal is then split. The first signal is counted by a Caen Quad Scaler N145. The second signal triggers the gate of a LeCroy ADC 2249A.

The gate duration has been set to 100 ns to take fully into account the time jitter, the pulse duration and the photon collections time (the prototype pulses typically exhibit rise times of few ns and fall times of ~ 10 ns).

The analog signal from the XP2020 PM (HV = 2100 V and Gain = 3×10^7) is amplified by a factor 10 by a LeCroy PM Amplifier 612A and then delayed and split. The first pulse is directly readout into the ADC. The other one is discriminated ($V_{th} = 20$ mV) and put in coincidence with a signal from the trigger gate line. This resulting pulse is then counted by the scaler.

By means of the scaler it has been possible to evaluate the trigger inefficiency. We have measured a geometrical inefficiency of $\sim 3\%$ and an electronic one of $\sim 1\%$.

3.2. Data analysis

The average number of detected photoelectrons has been evaluated according to the *PM spectrum method* [17]. This method is based on the analysis of the PM spectrum. It has to be pointed out that this method is reliable whenever the PM spectra clearly show the single photoelectron peak (see Fig. 3).

The analysis procedure consists of the following steps:

(1) The pedestal peak is fitted with a Gaussian distribution, to determine its mean (M_{ped}) and its variance (σ^2_{ped}).
(2) The contents of the channels from zero to $M_{ped} + 3\sigma_{ped}$ are set to zero. In this way the pedestal is completely erased, but a part of the signal is also lost.
(3) To recover the lost signal, a Gaussian fit of the single photoelectron (p.e.) peak is performed, and the previously suppressed values are replaced by Gaussian random values generated according to the fit parameters. If the single p.e. peak is not evident, the Gaussian fit is performed on the whole spectrum, giving a less accurate but still useful result.
(4) The average number of detected p.e. is calculated according to the formula:

$$\bar{n} = \frac{M_{dist} - M_{ped}}{CC} \quad (1)$$

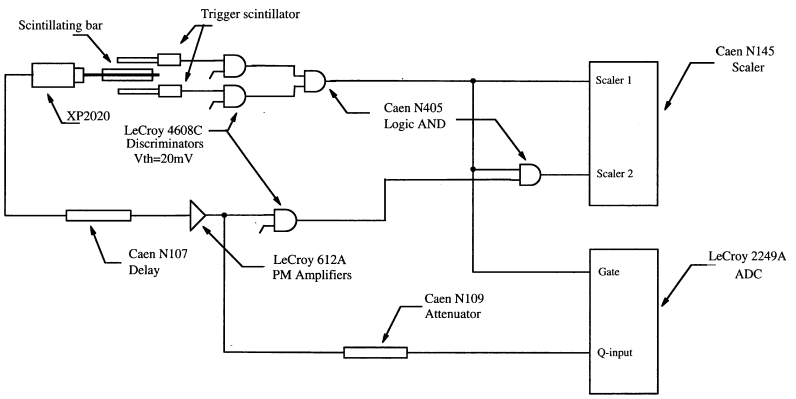

Fig. 2. Trigger layout.

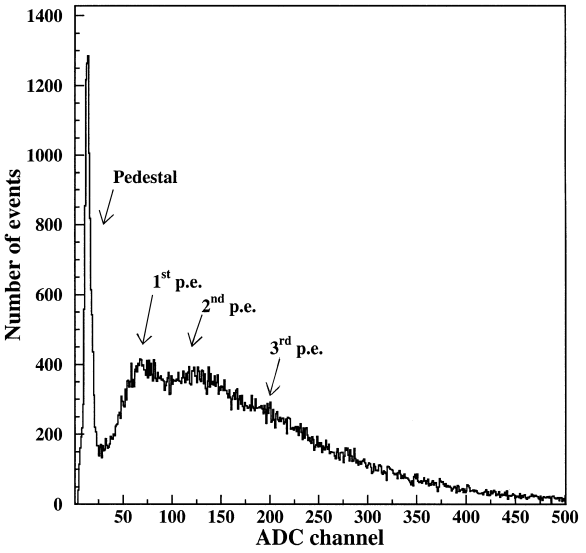

Fig. 3. Typical differential PM spectrum. The pedestal and the single p.e. peaks are evident. Also two p.e. peak is visible. We have to remark that the three peaks are equispaced.

where M_{dist} is the mean value of the recorded pedestal subtracted PM spectrum and CC is the calibration coefficient, i.e., the difference between the single and the double p.e. peaks expressed in ADC channels. This difference should be equal to the difference between the pedestal and single p.e. peaks. The CC parameter has been evaluated by using a measured spectrum where the pedestal, single and double p.e. peaks can be easily resolved (see Fig. 2). Its measured value is 50 ± 6 ch.

This method is always reliable, but its main drawback is that the results are strongly dependent on the fit interpolations. The uncertainty on $\bar{n}$ can be evaluated according to the following expression, obtained by applying the error propagation formula to Eq. (1):

$$\sigma_{\bar{n}} = \frac{1}{\mathrm{CC}}\sqrt{\sigma^2_{M_{\mathrm{dist}}} + \sigma^2_{M_{\mathrm{ped}}} + \left(\frac{M_{\mathrm{dist}} - M_{\mathrm{ped}}}{\mathrm{CC}}\right)^2 \sigma^2_{\mathrm{CC}}}. \tag{2}$$

Since the first two terms under the square root are by one-order of magnitude smaller than the third one, they can be safely neglected.

$$\sigma_{\bar{n}} \simeq 2.4 \times 10^{-3}(M_{\mathrm{dist}} - M_{\mathrm{ped}}). \tag{3}$$

4. Results

4.1. Attenuation length

We have measured the attenuation length of the WLS fiber by placing at different distances from PM, the trigger scintillators. In this case a 600 cm long Pol.Hi.Tech. scintillator was used. The optical glue used is Bicron BC 600. We have obtained quite similar results with the shorter scintillator bars (23 cm long).

In Fig. 4, we show the result both for an unmirrored and a mirrored fiber. We have used a diffuse reflector (TiO_2) to mirror the fiber end.

The reflector effect is evident only if the distance of the bar from the PM is greater than 2 m: the reflected photon path is quite similar to the direct photon path.

Experimental data have been fitted with the following function:

$$I(d) = I_0(\mathrm{e}^{-d/\lambda_1} + \alpha \mathrm{e}^{-d/\lambda_2}) \tag{4}$$

where λ_1 and λ_2 are, respectively, the attenuation lengths of the light trapped into the external cladding and of the light guided by internal reflection into the fiber core, and α is a parameter taking into account the relative weights of these processes. The data fitted results are in Table 3.

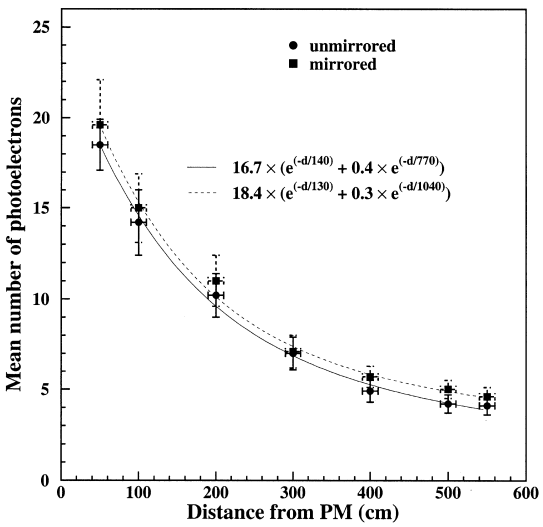

Fig. 4. Mean number photoelectrons versus distance.

Table 3
Attenuation lengths for mirrored and unmirrored fibers

Fiber type	λ_1 (m)	λ_2 (m)
Mirrored	1.3 ± 0.3	10.4 ± 1.3
Unmirrored	1.4 ± 0.3	7.7 ± 0.6

The reported attenuation length for the mirrored fiber is just a parameter used for comparison, since it does not represent the real attenuation length, that is correctly given by the following expression:

$$I(d) = I_0 \cdot ((e^{-d/\lambda_1} + \alpha e^{-d/\lambda_2}) + R(e^{-(2L-d)/\lambda_1} + \alpha e^{-(2L-d)/\lambda_2})) \quad (5)$$

where R is the reflection coefficient, L the fiber length and d the distance between the light production point and the fiber end. We can, however, mark that by mirroring a fiber end with a diffuse reflector, the light yield increases to $\sim 10\%$.

4.2. Light yield and efficiency

For the light yield and efficiency studies, two 600 cm Pol.Hi.Tech. scintillating bar with 1×4 cm^2 and 0.5×1 cm^2 cross-section have been used.

We have used a double readout (Fig. 5) to collect all the photons emitted by the WLS fiber. The two PM tubes have been previously calibrated with a light pulser, tuning HV to obtain the same gain.

The light yield for both the tested bars is shown in Fig. 6. As expected the smaller the cross-section (0.5×1 cm^2) the lower the light yield, since the path length of the crossing particle in the scintillating medium is shorter and consequently the ionization energy deposit, the number of produced and collected photons are lower.

A qualifying parameter is the light yield uniformity along all the fiber length. The longitudinal uniformity LU has been defined as

$$\mathrm{LU} = \frac{S}{M} \quad (6)$$

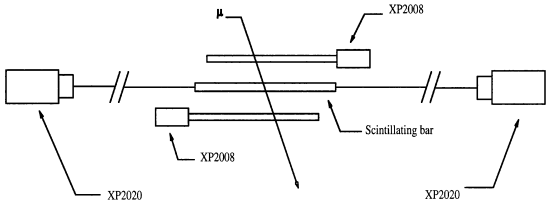

Fig. 5. Layout of double readout set-up.

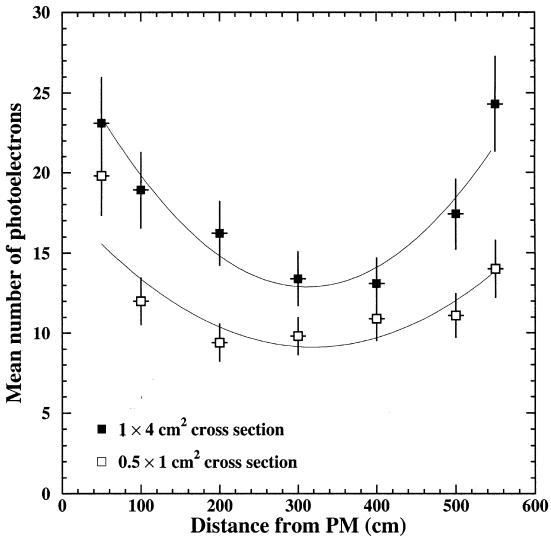

Fig. 6. Double readout light yield for both tested cross-section.

where M and S are the mean value and the RMS spread of the number of detected p.e., all along the fiber.

For the 1×4 cm^2 bar, the measured light yield uniformity is 16% (with the end points discarded) and for the thinner one is 14% (with the first point discarded). As expected, the longitudinal uniformity is not greatly affected by the bar cross-section since it is mainly due to the WLS fiber.

The light yield enhancement observed near the ends of the fiber is mainly due to short wavelength tail in the WLS fiber emission spectrum and to photons propagating in the external fiber cladding. An improvement in uniformity can be easily achieved by using UV filter in front of the PM and by painting the last 10 cm of the fiber black [18], to reduce the light propagation into the external cladding.

An interesting feature of the prototype is the global detection efficiency. The data collected with the 1×4 cm^2 cross-section bar show an almost uniform efficiency of $\simeq 85\%$, while for the thinner bar the detection efficiency is $\simeq 55\%$. This is due to a reduced light collection capability.

The energy resolutions for electrons and hadrons have been evaluated by GEANT 3.21 based on Monte Carlo code [9]. The detector simulation is performed by considering a fluctuation of about 15% around the measured attenuation length of the WLS fiber, and by assuming a mean value of 15 p.e. per m.i.p. and scintillator plane, according to the measured light yields. The energy resolutions obtained are $50\%/\sqrt{E}$ for hadrons and $17\%/\sqrt{E}$ for electrons that are consistent with the prefixed limits.

5. Conclusion

We have tested the main properties of a scintillating bar with WLS fiber readout in order to fully understand the behavior of this detector as active part of a sandwich calorimeter. We have measured an attenuation length of about 4 m and a light yield of 15 p.e. in the middle of a 6 m-long WLS fiber. The measured longitudinal uniformity is typically 15% The energy resolutions achievable in the framework of the NOE calorimeter design are $50\%/\sqrt{E}$ for hadrons and $17\%/\sqrt{E}$ for electrons.

References

[1] The SuperKamiokande Collaboration, Phys. Rev. 81 (1998) 1562.
[2] The MACRO Collaboration, Phys. Lett. B 434 (1998) 451.
[3] The Soudan2 Collaboration, Phys. Lett. B 449 (1999) 137.
[4] The ICANOE Collaboration, CERN/SPSC 99-25, INFN/AE 99-17, SPSC/P314, 1999.
[5] The MINOS Collaboration, NuMI-L-337, 1998.
[6] The MONOLITH Collaboration, LNGS-LOI 20/99, CERN/SPSC 99-24, SPSC/M636.
[7] The OPERA Collaboration, LNGS-LOI 19/99, CERN/SPSC 99-20, SPSC/M635.
[8] R.J. Wilkes et al., in: T. Donnelly (Ed.), Proceedings of the Sixth Conference On the Intersections Between Particle and Nuclear Physics, AIP Conference Proceedings Vol. 412, AIP, New York, 1997, p. 311.
[9] The NOE Collaboration, INFN/AE-98/09 (1998).
[10] CNGS Conceptual Technical Design, CERN 98-02, INFN/AE-98/05.
[11] The ICARUS Collaboration, LNGS-94/99,LNGS-95/10,CERN/SPSLC/P304.
[12] The MACRO Collaboration, Phys. Rev. D46 (1992) 895.
[13] The MAC Collaboration, Proceedings of the International Conference on Instrumentation for Colliding Beam Physics, 1982, SLAC-R-250.
[14] S. Buontempo et al., Nucl. Instr. and Meth. A 349 (1994) 70.
[15] K.V. Alexandrov et al., Nucl. Instr. and Meth. A 456 (2000) 259.
[16] POL.HI.TECH., Carsoli, L'Aquila, Italy.
[17] J.P. O'Callaghan et al., Nucl. Instr. and Meth. A 225 (1984) 153.
[18] S. Buontempo et al., Nucl. Instr. and Meth. A 349 (1994) 70.